Inhibition of SAT1 alleviates chondrocyte inflammation and ferroptosis by repressing ALOX15 expression and activating the Nrf2 pathway

Cite this article:
Bone Joint Res 2024;13(3):
110–123.

DOI: 10.1302/2046-3758.
133.BJR-2023-0250.R1

Correspondence should be sent to Fengjing Guo
guofjdoc@163.com

J. Xu,[1] Z. Ruan,[1] Z. Guo,[1] L. Hou,[1] G. Wang,[1] Z. Zheng,[1] X. Zhang,[1] H. Liu,[1] K. Sun,[1] F. Guo[1]

Department of Orthopedics, Tongji Hospital, Tongji Medical College, Huazhong University of Science and Technology, Wuhan, China

Aims

Osteoarthritis (OA) is the most common chronic pathema of human joints. The pathogenesis is complex, involving physiological and mechanical factors. In previous studies, we found that ferroptosis is intimately related to OA, while the role of Sat1 in chondrocyte ferroptosis and OA, as well as the underlying mechanism, remains unclear.

Methods

In this study, interleukin-1β (IL-1β) was used to simulate inflammation and Erastin was used to simulate ferroptosis in vitro. We used small interfering RNA (siRNA) to knock down the spermidine/spermine N1-acetyltransferase 1 (Sat1) and arachidonate 15-lipoxygenase (Alox15), and examined damage-associated events including inflammation, ferroptosis, and oxidative stress of chondrocytes. In addition, a destabilization of the medial meniscus (DMM) mouse model of OA induced by surgery was established to investigate the role of Sat1 inhibition in OA progression.

Results

The results showed that inhibition of Sat1 expression can reduce inflammation, ferroptosis changes, reactive oxygen species (ROS) level, and lipid-ROS accumulation induced by IL-1β and Erastin. Knockdown of Sat1 promotes nuclear factor-E2-related factor 2 (Nrf2) signalling. Additionally, knockdown Alox15 can alleviate the inflammation-related protein expression induced by IL-1β and ferroptosis-related protein expression induced by Erastin. Furthermore, knockdown Nrf2 can reverse these protein expression alterations. Finally, intra-articular injection of diminazene aceturate (DA), an inhibitor of Sat1, enhanced type II collagen (collagen II) and increased Sat1 and Alox15 expression.

Conclusion

Our results demonstrate that inhibition of Sat1 could alleviate chondrocyte ferroptosis and inflammation by downregulating Alox15 activating the Nrf2 system, and delaying the progression of OA. These findings suggest that Sat1 provides a new approach for studying and treating OA.

Article focus

- Focus on the function of spermidine/spermine N1-acetyltransferase 1 (Sat1)–arachidonate 15-lipoxygenase (Alox15) axis in the progression of osteoarthritis (OA).

Key messages

- Knockdown of Sat1 and Alox15 can reduce chondrocyte inflammation and ferroptosis.
- The Sat1-Alox15 axis regulated nuclear factor-E2-related factor 2 (Nrf2) signalling in chondrocytes.

Bone & Joint Research

- Diminazene aceturate (DA) inhibited Sat1 expression to protect chondrocytes; DA also alleviated cartilage degeneration and increased the expression of type II collagen in the mouse OA model.

Strengths and limitations

- The role of the Sat1-Alox15 axis in OA progression was revealed for the first time.
- We established a connection between Nrf2 and Sat1-Alox15 in the OA model.
- The study lacked experimental evidence for human cells.

Introduction

Osteoarthritis (OA) is the most common degenerative joint disease in humans. The disease is closely related to age. The main features are more severe in synovial tissue, articular cartilage, subchondral bone, and osteophyte formation.[1] With the combined impact of ageing and increasing obesity, this kind of syndrome has caused increasing burdens worldwide.[2] In recent years, researchers have considered OA to be a complicated disease mediated by inflammation, catabolism, and many other factors.[3-7] Among these corresponding factors, inflammation is the main factor related to cartilage loss and disease symptoms.[8]

As a unique factor in cartilage, chondrocytes maintain the balance of the extracellular matrix (ECM) through anabolism and catabolism.[9,10] The dysfunction of chondrocytes makes a significant contribution to the progression of OA. Research has shown that chondrocyte damage can be caused by necrosis, apoptosis, and autophagy.[11] In 2012, Dixon et al[12] discovered a new mode of cellular demise named ferroptosis that differed from other forms. Ferroptosis is defined as iron-dependent cellular demise caused by oxidation disorders of the intracellular microenvironment and lipid reactive oxygen species (ROS) accumulation.[13]

Previous studies demonstrated that chondrocytes undergo ferroptosis under inflammatory conditions and that ferroptosis is related to the progression of OA.[14,15] SLC7A11 is a subunit of the cystine/glutamate reverse transporter, which can reduce glutathione (GSH) release and lipid peroxidation in cells.[16] P53, a cancer suppressor gene, plays a crucial role in ferroptosis by inhibiting SLC7A11 and regulating apoptosis.[17] Spermidine/spermine N1-acetyltransferase 1 (Sat1), which is downstream of P53, plays a significant role in the rate-limiting enzyme associated with polyamine catabolism and induces lipid peroxidation and ferroptosis through ROS and lipid ROS.[18] Arachidonate 15-lipoxygenase (Alox15) is considered to be the central participant in ferroptosis, and can effectively oxidize various phosphatidylethanolamines into iron-reducing signalling molecules.[19] Nuclear factor-E2-related factor 2 (Nrf2) plays an antioxidant and anti-inflammatory role in OA chondrocytes by regulating cellular redox status,[20,21] and its signal pathway activator has been proven to protect experimental models of various chronic diseases.[22] However, the role of the Sat1-Alox15 pathway in OA is still unclear.

In this study, we aimed to investigate the role of Sat1 in chondrocyte ferroptosis and verify whether the Alox15-Nrf2 axis mediates the action of Sat1.

Methods

Reagents

Diminazene aceturate (DA) was acquired from Selleckchem (USA). Interleukin-1β (IL-1β) (# 401-ML) was acquired from R&D systems (USA). Erastin (S7242) was acquired from Selleckchem (USA). ROS assay kit (S0033) was provided by Beyotime (China). Sat1 (10708-1-AP, diluted 1:5000), Nrf2 (U16396-1-AP, diluted 1:5,000), HO-1 (10701-1-AP, diluted 1:5,000), type II collagen (collagen II) (28459-1-AP, diluted 1:2,000), matrix metalloproteinase 13 (MMP13) (18165-1-AP, diluted 1:5,000), MMP3 (17873-1-AP, diluted 1:5000), inducible nitric oxide synthase (iNOS) (22226-1-AP, diluted 1:5000), and glyceraldehyde 3-phosphate dehydrogenase (GAPDH) antibodies (60004-1-Ig, diluted 1:5,000) were acquired from Proteintech (USA). Alox15 (A6865, diluted 1:5000) and lpcat3 antibodies (A17604, diluted 1:1000) were acquired from Abclonal (China). Glutathione peroxidase 4 (GPX4) (ab125066, diluted 1:5,000), SLC7A11 (ab175186, diluted 1:5,000), and NAD(P)H:quinone oxidoreductase 1 (NQO1) antibodies (ab80588, diluted 1:1,000) were acquired from Abcam (UK). The C11 BODIPY Sensor (D3861) was acquired from Thermo Fisher Scientific (USA). The Micro Malondialdehyde (MDA) assay kit (BC0025) was acquired from Solarbio (China).

Isolation and culture of murine chondrocytes

Chondrocytes were separated from five-day-old C57BL/6J mice.[23] After removal from the knee joints, the cartilage was cut and digested with 0.25% trypsin and 0.25% collagenase. Primary chondrocytes were resuspended, collected, and cultured in Dulbecco's Modified Eagle Medium (DMEM)/F12 medium containing 10% fetal bovine serum (FBS) in a humid atmosphere at 37°C with 5% CO_2. The cells were subcultured at 80% confluence and transferred to culture bottles. Chondrocytes in the first and second generations were applied in our study.

Western blot

Chondrocytes were inoculated into six-well plates at a density of 5×10^5 cells per well and allowed to adhere for 48 hours. First, the cells were treated in different groups for 24 hours. The cells were washed twice with phosphate-buffered saline (PBS), and then RIPA lysis buffer containing a 1% protease inhibitor mixture (AR0102; Boster, China) was used to lyse chondrocytes for 30 minutes on ice. The extract was collected and subjected to centrifugation at a speed of 12,000× g and a temperature of 4°C for 30 minutes. Then, a BCA analysis kit (AR0146; Boster) was used to determine the protein concentration of cell lysates. Next, the supernatant of each sample was collected, and then the samples (25 μg) were separated through electrophoresis on a 12% SDS-PAGE gel and transferred to polyvinylidene difluoride (PVDF) membrane (MilliporeSigma, USA). After being blocked with 5% skimmed milk at ordinary temperature for one hour, the membranes and specific primary antibodies were incubated at 4°C overnight. Subsequently, the membranes were incubated with secondary antibodies at room temperature for one hour. To visualize the protein bands, ultra-sensitive ECL chemiluminescence reagent from Boster was employed. The resulting images were captured using the ChemiDocTM XRS+ System (Bio-Rad Laboratories, USA).

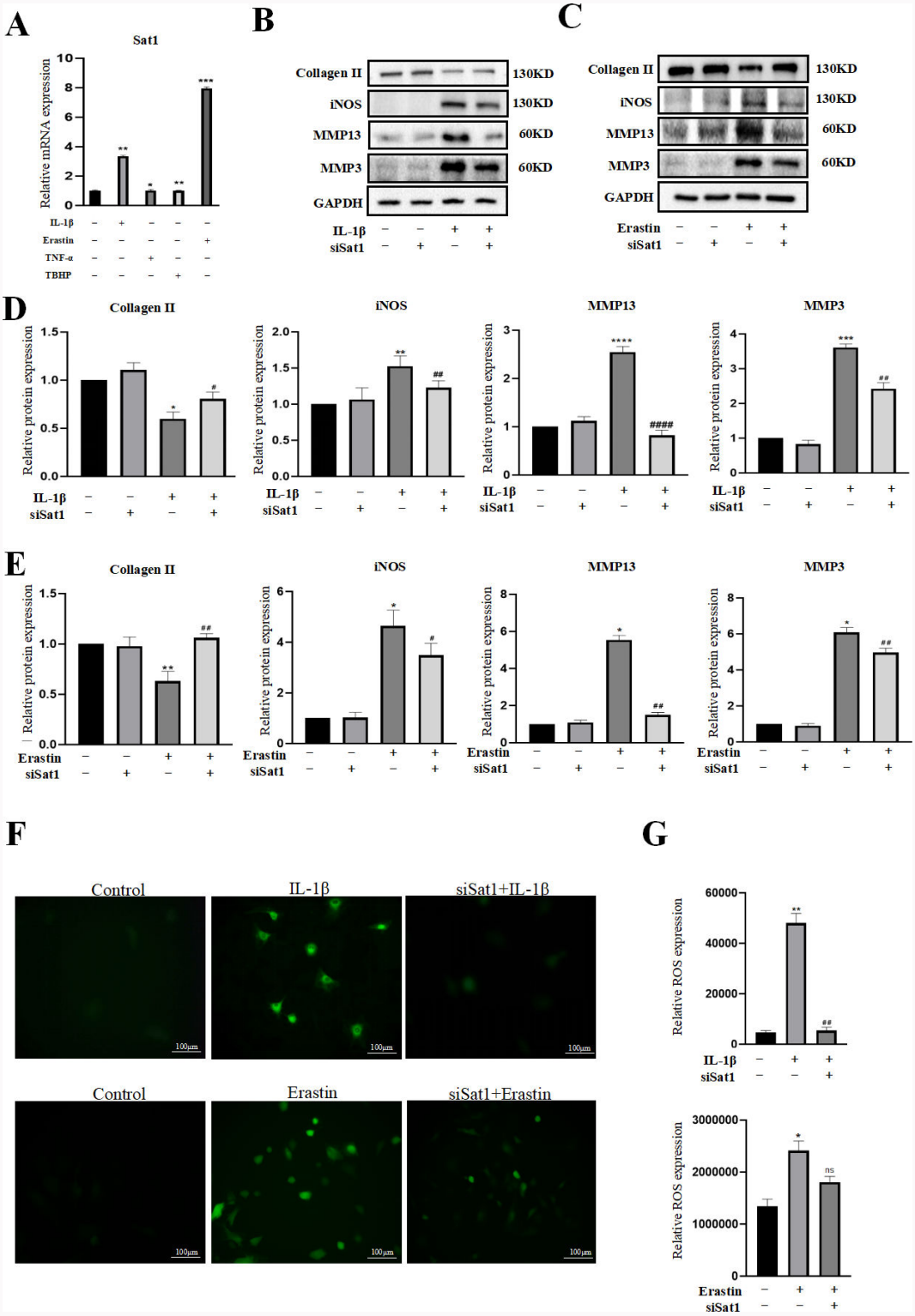

Fig. 1

Interleukin-1β (IL-1β)- and Erastin-induced changes in expression of inflammatory proteins in chondrocytes, which could be prevented by spermidine/spermine N1-acetyltransferase 1 (Sat1) knockdown. a) Sat1 expression changed in chondrocytes induced by IL-1β, Erastin, tumour necrosis factor-α (TNF-α), and tert-butyl hydroperoxide (TBHP), as detected by quantitative polymerase chain reaction (qPCR). b) to e) Western blot analysis was conducted to detect the protein expression levels of type II collagen (collagen II), inducible nitric oxide synthase (iNOS), matrix metalloproteinase 13 (MMP13), and MMP3 following treatment with IL-1β (10 ng/ml) or Erastin (5 μM), and to quantify the band density ratios of collagen II, iNOS, MMP13, and MMP3 to glyceraldehyde 3-phosphate dehydrogenase (GAPDH) (experiments repeated three times each). f) and g) The intracellular level of reactive oxygen species (ROS) was evaluated using the DCFH-DA fluorescent probe (scale bar: 100 μm). These data were statistically analyzed by independent-samples *t*-test and are presented as the mean and standard deviation. *p < 0.05 vs the negative control group. #p < 0.05 vs the IL-1β group or Erastin group.**p < 0.005, ***p < 0.0005, ****p < 0.0001. DA, diminazene aceturate; mRNA, messenger RNA; ns, non-significant.

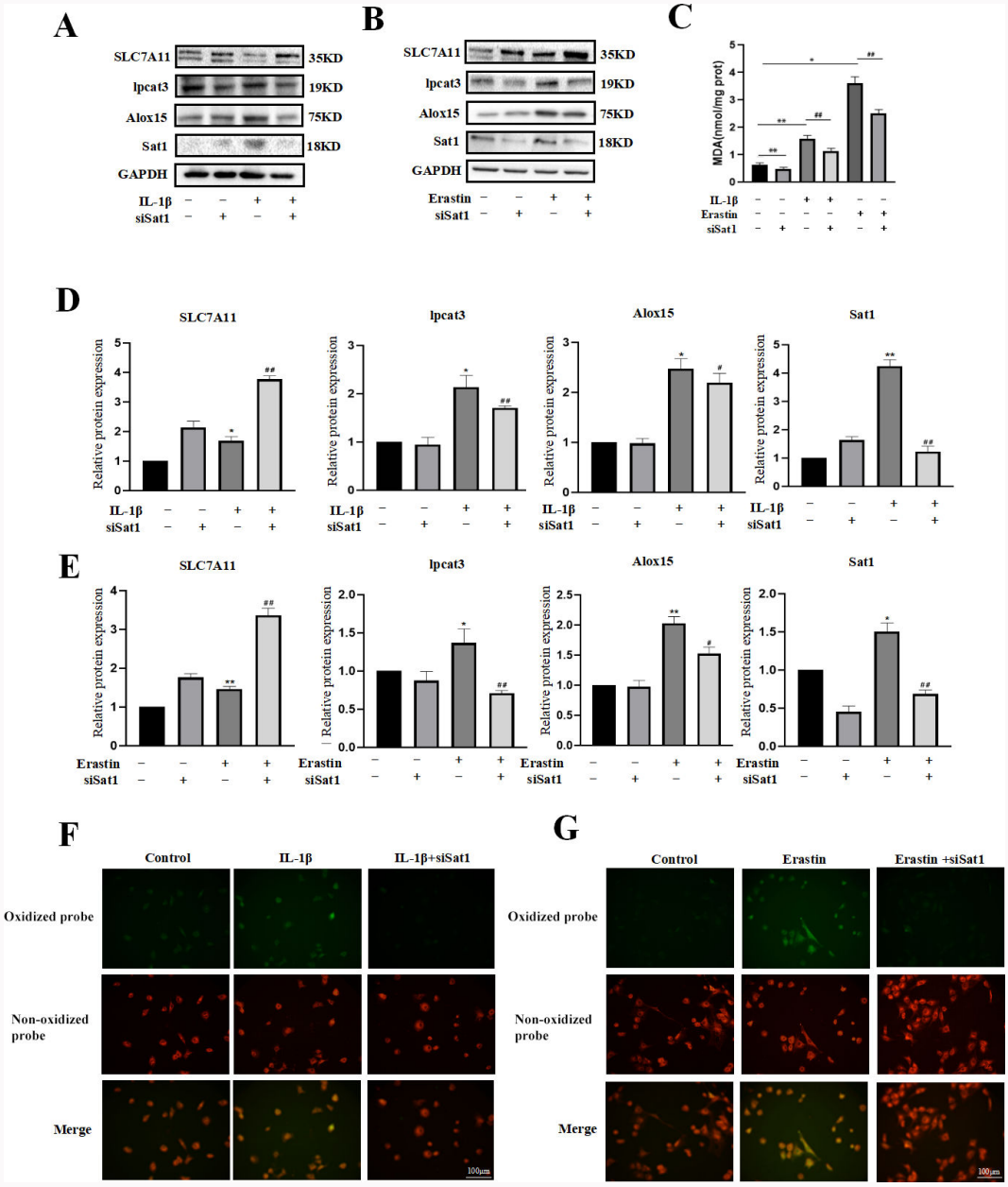

Fig. 2

Treatment with interleukin-1β (IL-1β) and Erastin led to the accumulation of reactive oxygen species (ROS) and alterations in the expression of proteins associated with ferroptosis in chondrocytes. These effects can be reversed by silencing spermidine/spermine N1-acetyltransferase 1 (Sat1). a) and b) Western blot analysis was conducted to detect the protein expression levels of SLC7A11, Ipcat3, arachidonate 15-lipoxygenase (Alox15), and Sat1 in chondrocytes following treatment with IL-1β (10 ng/ml) or Erastin (5 μM), with the chondrocytes transfected with siSat1. c) The malondialdehyde (MDA) assay kit was employed to measure the intracellular levels of MDA (experiments repeated three times each). d) and e) Densitometry analysis was used to quantify the band density ratios of SLC7A11, Ipcat3, Alox15, and Sat1 to glyceraldehyde 3-phosphate dehydrogenase (GAPDH) (experiments repeated three times each). f) and g) Lipid-ROS measured by C11 BODIPY fluorescent probe. The red portion of C11-BODIPY represents its reduced form, while the green portion represents its oxidized form (scale bar: 100 μm). These data were statistically analyzed by independent-samples *t*-test and are presented as the mean and standard deviation. *p < 0.05 vs the negative control group. #p < 0.05 vs the IL-1β group or Erastin group. **p < 0.005.

Quantitative reverse transcription polymerase chain reaction

Total RNA extraction was performed using the Total RNA extration Kit (Omega Bio-tek, UK). The First Strand cDNA Synthesis Kit (Yeasen, China) was used to synthesize complementary DNA (cDNA) from total RNA. Next, the cDNA was amplified with SYBR Green Realtime PCR Master Mix (Yeasen, China) using the following cycling conditions: 30 seconds of polymerase activation at 95°C, followed by 40 cycles of 95°C for five seconds and 60°C for 30 seconds. Internal control was GAPDH. cDNA samples were run in triplicate. The primer sequences used were: Sat1-forward (TGACCCATGGATTGGCAAGT); and Sat1-reverse (CAGCGACACTTCATGGCAAC).

Toluidine blue staining

Chondrocytes were inoculated into 36 mm culture dishes. The cells were washed with PBS three times and mixed with 4% paraformaldehyde for 30 minutes. Then, the cells

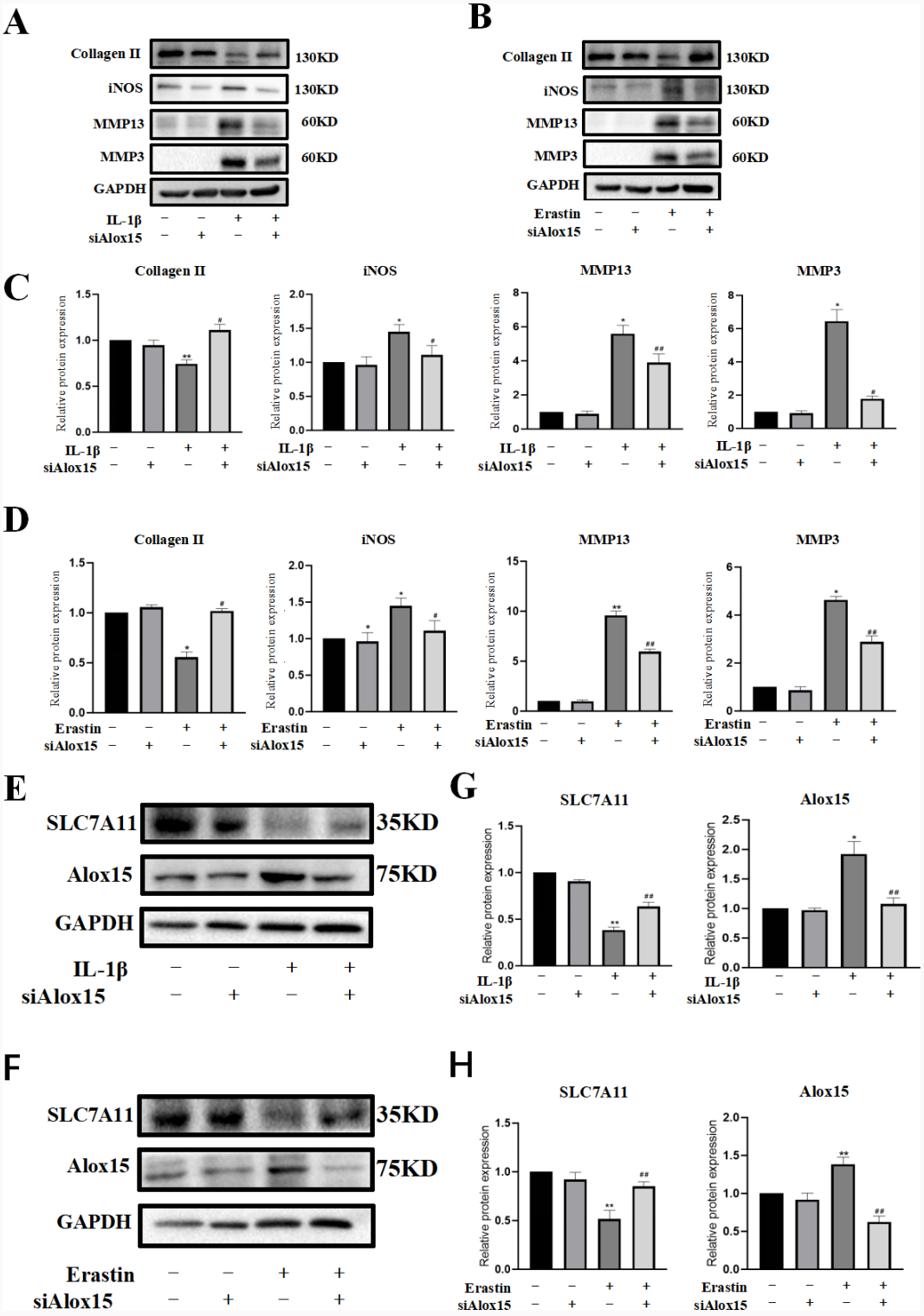

Fig. 3

Knockdown of arachidonate 15-lipoxygenase (Alox15) can effectively protect chondrocytes from inflammation and ferroptosis. a) to d) Western blot analysis was conducted to detect the protein expression levels of type II collagen (collagen II), iNOS, matrix metalloproteinase 13 (MMP13), and MMP3 in chondrocytes following treatment with interleukin-1β (IL-1β) (10 ng/ml) or Erastin (5 μM), as well as being subjected to Alox15 knockdown. Densitometry was performed to quantify the band density ratios of collagen II, MMP13, and MMP3 to glyceraldehyde 3-phosphate dehydrogenase (GAPDH) (experiments repeated three times each). e) to h) Western blot analysis was conducted to detect the protein expression levels of SLC7A11 and Alox15 in chondrocytes treated with IL-1β (10 ng/ml) or Erastin (5 μM) and subjected to Alox15 knockdown. Densitometry analysis was performed to quantify the band density ratios of SLC7A11 and Alox15 to GAPDH in the western blots (experiments repeated three times each). These data were statistically analyzed by independent-samples *t*-test and are presented as the mean and standard deviation. *p < 0.05 vs the negative control group. #p < 0.05 vs the IL-1β group or Erastin group. **p < 0.005.

were incubated with toluidine blue for 24 hours. Finally, the redundant dye was removed, and the cells were washed with

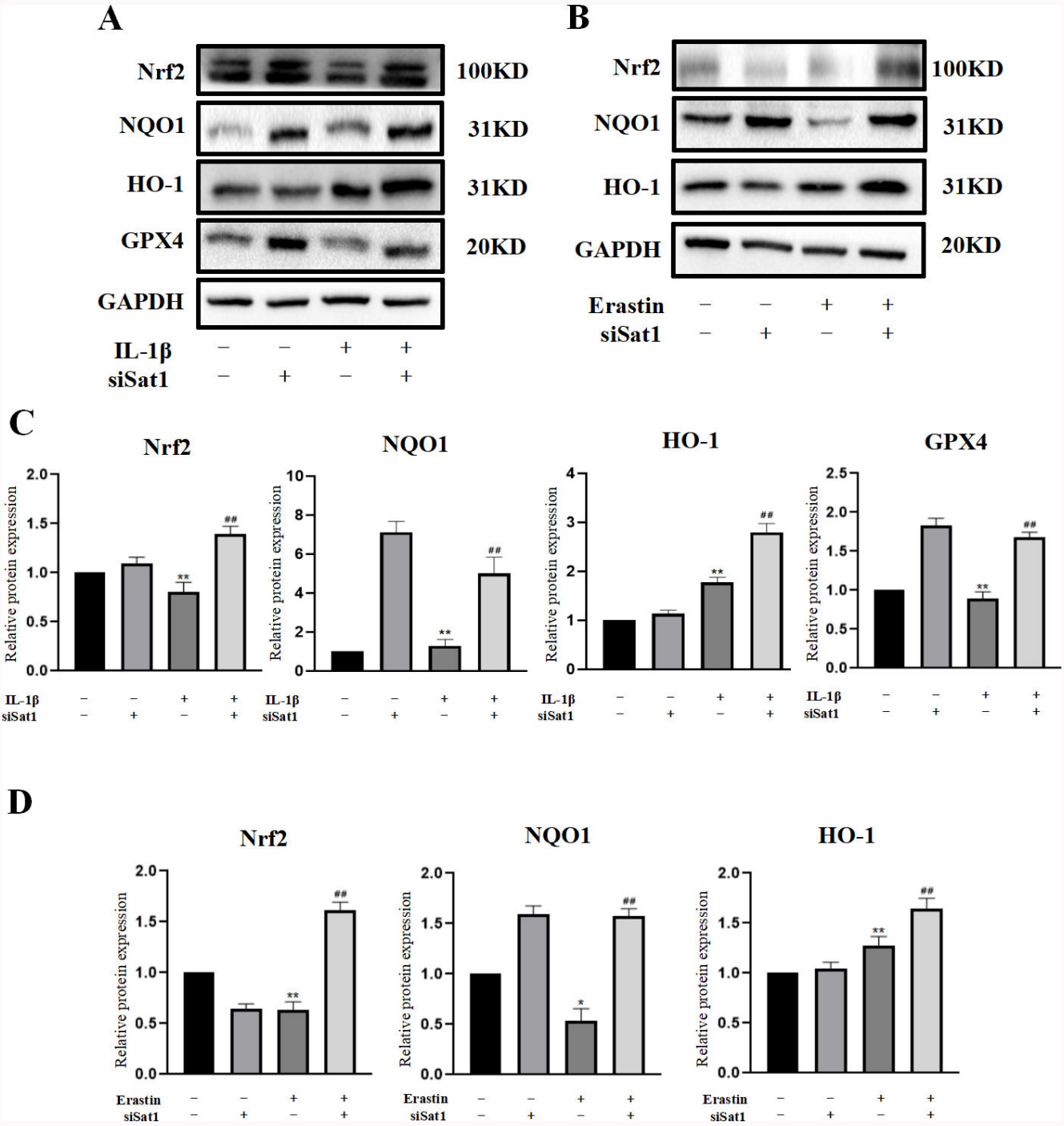

Fig. 4

Antioxidation of nuclear factor-E2-related factor 2 (Nrf2) axis on chondrocytes induced by interleukin-1β (IL-1β) or Erastin increased after spermidine/spermine N1-acetyltransferase 1 (Sat1) knockdown. a) and b) Western blot analysis was conducted to detect the protein expression levels of Nrf2, NAD(P)H:quinone oxidoreductase 1 (NQO1), Heme Oxygenase-1 (HO-1), and glutathione peroxidase 4 (GPX4) in chondrocytes treated with IL-1β (10 ng/ml) or Erastin (5 μM) and subjected to Sat1 knockdown. c) and d) Densitometry analysis was conducted to quantify the band density ratios of Nrf2, NQO1, HO-1, and GPX4 to glyceraldehyde 3-phosphate dehydrogenase (GAPDH) in the western blots (experiments repeated three times each). These data were statistically analyzed by independent-samples *t*-test and are presented as the mean and standard deviation. *$p < 0.05$ vs the negative control group. #$p < 0.05$ vs the IL-1β group or Erastin group. **$p < 0.005$.

PBS three times. Then, the morphological changes of the chondrocytes were observed under a microscope (EVOS FL Auto; Life Technologies, Thermo Fisher Scientific).

Cell viability assay

Chondrocytes were inoculated into 96-well plates. Following a 24-hour treatment period, the medium was subsequently removed. Then, each well was supplemented with 100 μl of a 10% CCK-8 solution, followed by an incubation period of one hour at 37°C in a light-restricted environment. A microplate reader (Thermo Fisher Scientific, Finland) was used to determine the absorbance at 450 nm.

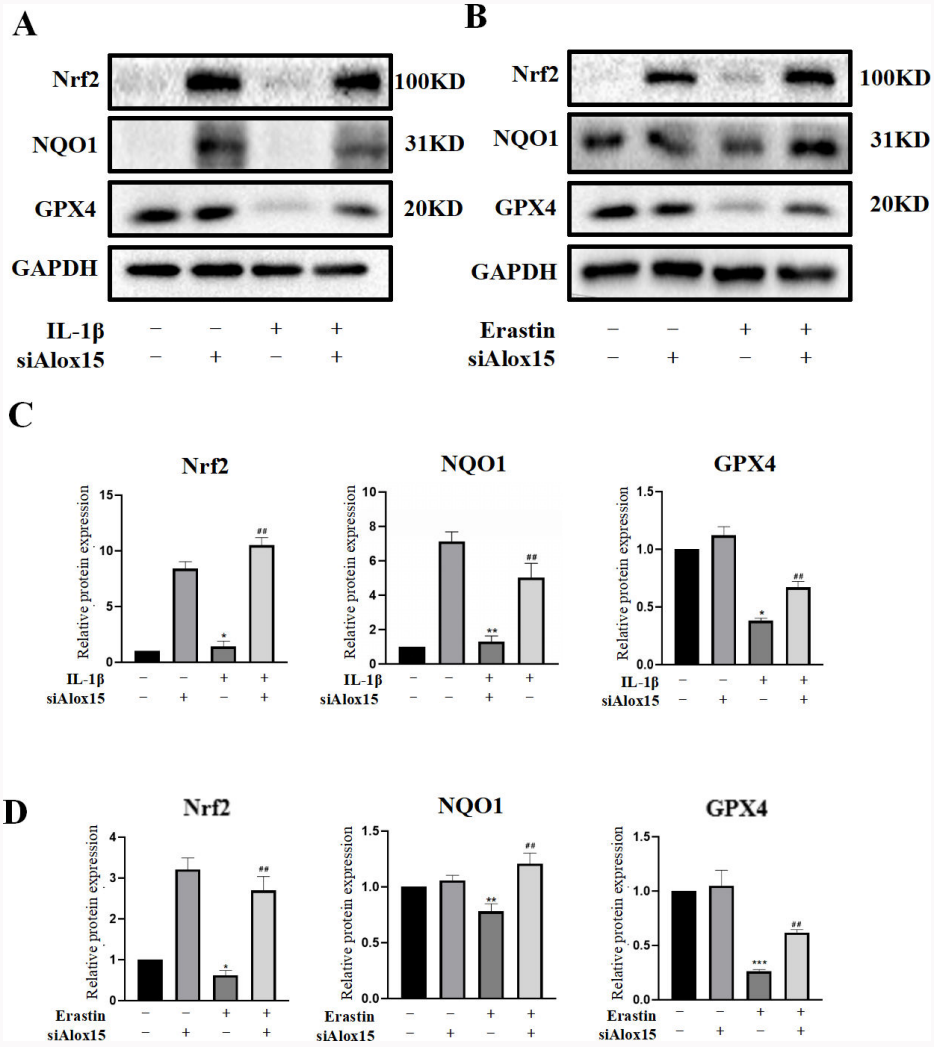

Fig. 5

Protective effect of nuclear factor-E2-related factor 2 (Nrf2) signalling on chondrocytes induced by interleukin-1β (IL-1β) or Erastin increased after arachidonate 15-lipoxygenase (Alox15) knockdown. a) to d) Western blot analysis was conducted to detect the protein expression of Nrf2, NAD(P)H:quinone oxidoreductase 1 (NQO1), and glutathione peroxidase 4 (GPX4) in chondrocytes treated with IL-1β (10 ng/ml) or Erastin (5 μM) and subjected to Alox15 knockdown. Densitometry analysis was conducted to quantify the band density ratios of Nrf2, NQO1, and GPX4 to glyceraldehyde 3-phosphate dehydrogenase (GAPDH) (experiments repeated three times each). These data were statistically analyzed by independent-samples *t*-test and are presented as the mean and standard deviation. *p < 0.05 vs the negative control group. #p < 0.05 vs the IL-1β group or Erastin group. **p < 0.005 .

Measured value of intracellular ROS and lipid ROS

Chondrocytes were inoculated in six-well plates. After being separated into the different treatment groups for 24 hours, the chondrocytes underwent three rounds of washing with PBS, after which they were exposed to 10 μM H2DCFDA (DCFH-DA) or 10 μM BODIPY 581/591 C11 (C11-BODIPY) at 37°C. Following PBS washing, the cells were examined under a fluorescence microscope (EVOS FL Auto). C11-BODIPY showed red fluorescence at 561 nm and green fluorescence at 488 nm.

Malondialdehyde assay

The MDA-TBA adduct composed of MDA and thiobarbituric acid (TBA) performed fluorescence measurements at excitation wavelengths of 532 nm and emission wavelengths of 553 nm.

Knockdown of Sat1, Alox15, and Nrf2 by siRNA

Specific small interfering RNA (siRNA) targeting the mouse Sat1 and Nrf2 genes was synthesized by RiboBio (China). Specific siRNA targeting the mouse Alox15 gene was synthesized by Puyun Biotechnology (China). Cells were transfected with Lipofectamine 3000 (Thermo Fisher Scientific) transfection reagent.

The Sat1 siRNA sense strand sequence was 5'-GGAATGA ACCATCTATCAA-3′, the Alox15 siRNA sense strand sequence was 5'-GCGAUUUCGAGAGGACAAA-3′, and the Nrf2 siRNA sense strand sequence was 5'-CGACAGACCCTCCATCTA-3′.

Animal experiment

All the animal experiments in this study adhered to the ARRIVE guidelines, and we have included an ARRIVE checklist to show this. Destabilization of the medial meniscus (DMM) was induced surgically in the right knee of an eight-week-old male C57BL/6J mouse to establish an experimental OA model, and

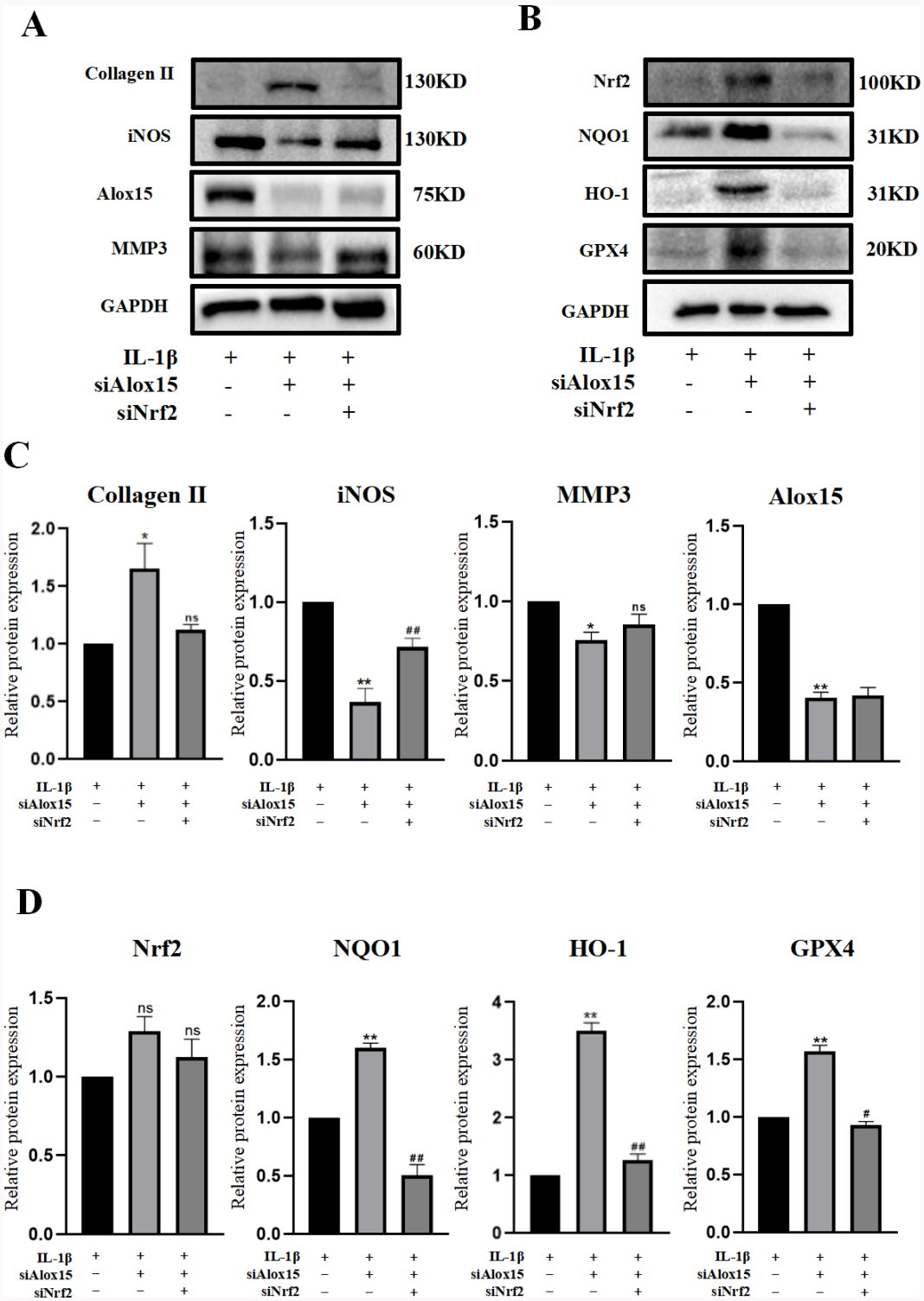

Fig. 6

Knockdown of nuclear factor-E2-related factor 2 (Nrf2) can reverse the therapeutic effect caused by arachidonate 15-lipoxygenase (Alox15) inhibition. a) and b) Western blot analysis was conducted to detect the protein expression of type II collagen (collagen II), iNOS, Alox15, matrix metalloproteinase 13 (MMP3), Nrf2, NAD(P)H:quinone oxidoreductase 1 (NQO1), Heme Oxygenase-1 (HO-1), and glutathione peroxidase 4 (GPX4) in chondrocytes treated with interleukin-1β (IL-1β) (10 ng/ml) and subjected to Alox15 and Nrf2 knockdown. c) and d) Densitometry analysis was used to quantify the band density ratios of collagen II, iNOS, Alox15, MMP3, Nrf2, NQO1, HO-1, and GPX4 to glyceraldehyde 3-phosphate dehydrogenase (GAPDH) (experiments repeated three times each). These data were statistically analyzed by independent-samples *t*-test and are presented as the mean and standard deviation. *p < 0.05 vs the negative control group. #p < 0.05 vs the IL-1β group or Erastin group. **p < 0.005 .

pentobarbital (36 mg/kg) was intraperitoneally injected for anesthesia. A total of 32 mice were randomly allocated into four groups: the sham group, DMM group, DMM + 3 mg/kg DA group, and DMM + 30 mg/kg DA group (n = 8 for each group). The mice were treated with DA (3 or 30 mg/kg) by intra-articular injection. Mice in the sham group and DMM group were treated with the same volume of double distilled water (ddH_2O) by intra-articular injection. The injections were

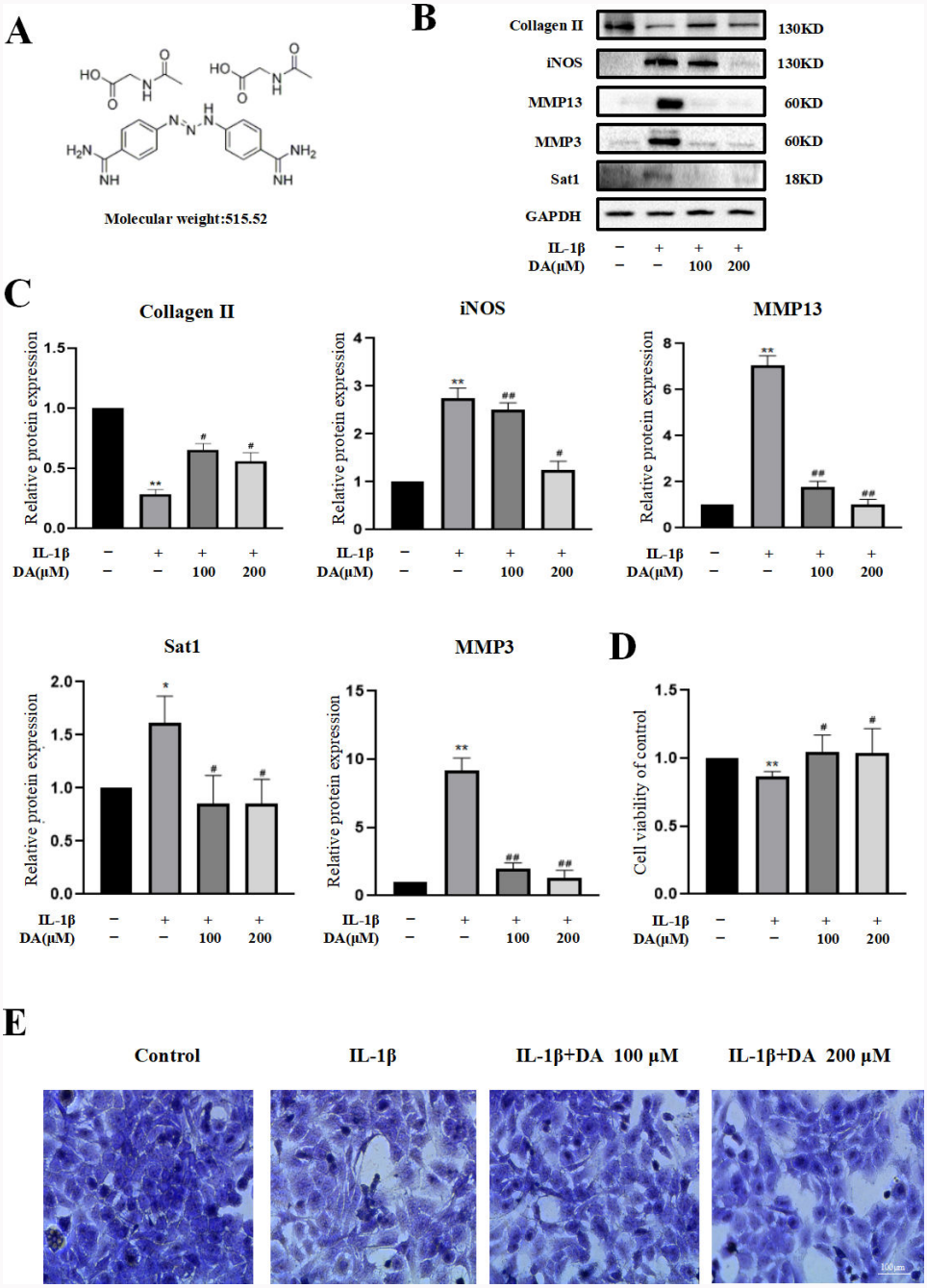

Fig. 7

Effect of diminazene aceturate (DA) on chondrocytes. a) Molecular weight and chemical structure of DA. b) and c) Western blot analysis was conducted to detect the expression of type II collagen (collagen II), iNOS, MMP13, MMP3, and arachidonate 15-lipoxygenase (Alox15) when treated with interleukin-1β (IL-1β) (10 ng/ml) and 100 or 200 μM DA or isochoric ddH_2O. Densitometry analysis was performed to quantify the band density ratios of collagen II, INOS, matrix metalloproteinase 13 (MMP13), MMP3, and Alox15 to glyceraldehyde 3-phosphate dehydrogenase (GAPDH) (experiments repeated three times each). d) Cell viability was determined through cell counting kit (CCK)-8 assay. e) Morphology and structure of the nucleus and cytoplasm determined by toluidine blue staining (scale bar: 100 μm). These data were statistically analyzed by independent-samples *t*-test and are presented as the mean and standard deviation. *p < 0.05 vs the negative control group. #p < 0.05 vs the IL-1β group. **p < 0.005 .

repeated twice per week for eight successive weeks. After eight weeks, the mice were euthanized, and the right knee joints were collected and fixed with 4% paraformaldehyde for subsequent experiments.

Immunohistochemical staining

The right knee joints were decalcified with 10% ethylenediaminetetraacetic acid (EDTA) for four weeks and embedded in paraffin wax. The specimens were sliced sagittally into sections with a thickness of 5 μm, followed by staining with safranin-O/fast green. The assessment of OA progression was carried out in a blinded manner. JX, ZR, and ZG assessed and averaged the Osteoarthritis Research Society International (OARSI)[24] score for further analysis. Furthermore, other sections were subjected to incubation with antibodies against Sat1, Alox15, MMP13, or collagen II. These sections were then stained using diaminobenzidine (DAB) and counterstained

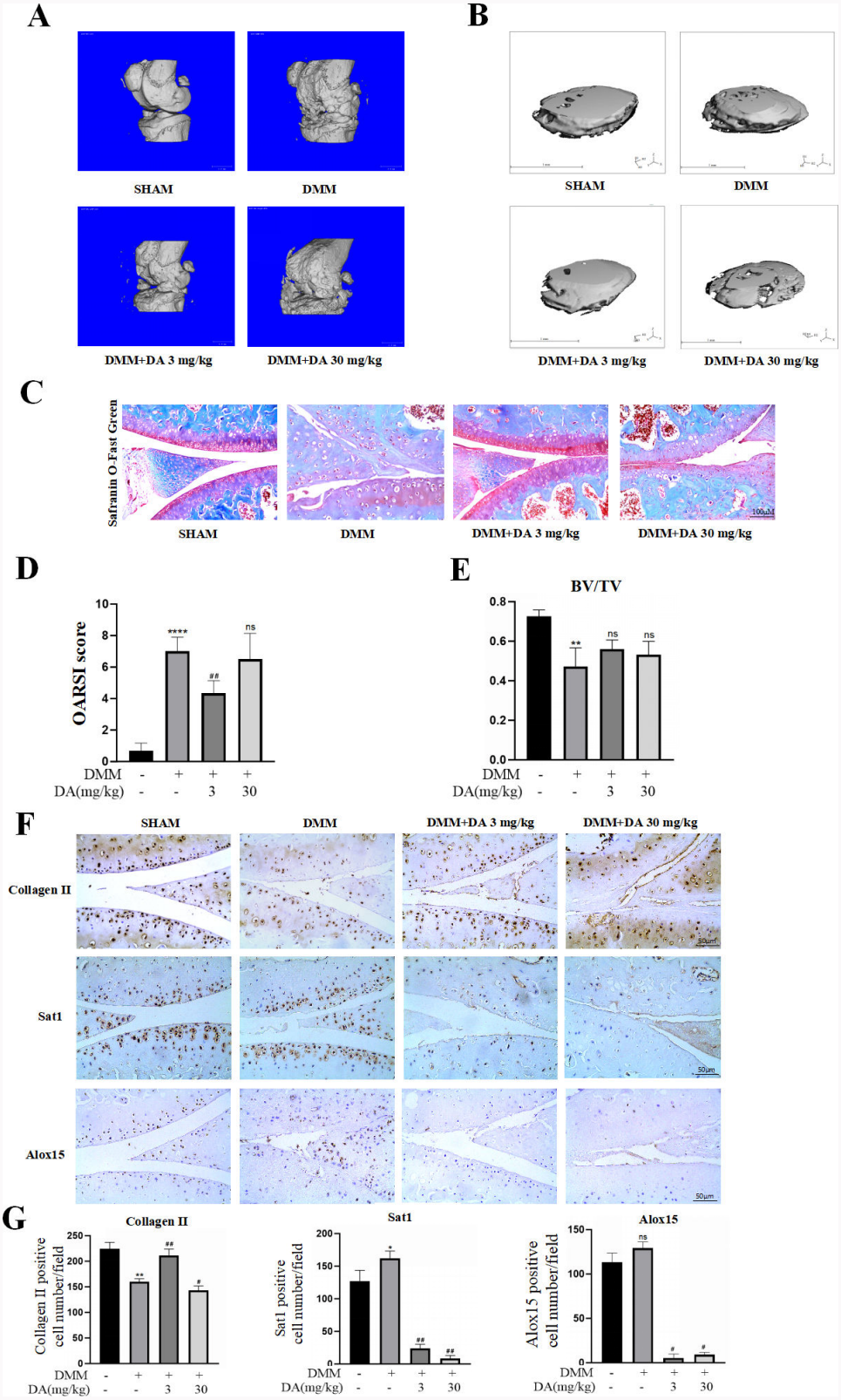

Fig. 8

Low concentrations of diminazene aceturate (DA) alleviated chondrocyte ferroptosis and osteoarthritis (OA) progress. a) Osteophyte formation was analyzed by micro-CT in C57 with DA (3 mg/kg or 30 mg/kg) treatment. b) Integrity of tibial plateau was analyzed by micro-CT in C57 with DA (3 mg/kg or 30 mg/kg). c) Degree of cartilage degradation was evaluated by safranin O/fast green staining (scale bar: 100 μm). d) Osteoarthritis Research Society International (OARSI) scores were used to evaluate the progression of OA (n = 8). e) Bone volume fraction (BV/TV) was measured in the tibial plateau of C57 after destabilization of the medial meniscus (DMM) surgery (n = 8). f) and g) Immunohistochemistry staining was used to measure the expression levels of type II collagen (collagen II), spermidine/spermine N1-acetyltransferase 1 (Sat1), and arachidonate 15-lipoxygenase (Alox15) in the cartilage samples (scale bar: 50 μm). These data were statistically analyzed by independent-samples *t*-test and are presented as the mean and standard deviation. *p < 0.05 vs the negative control group. #p < 0.05 vs the DMM group. **p < 0.005 .

with haematoxylin. Images were captured using a fluorescence microscope in a bright field (EVOS FL Auto).

Statistical analysis

All experiments were independently performed and repeated three times. Statistics were analyzed using GraphPad Prism 8.0 (GraphPad Software, USA). The results are expressed as means and standard deviations. The independent-samples *t*-test was used to compare differences between any two groups. One-way analysis of variance (ANOVA) was used to determine the differences among the two groups. P-values < 0.05 were considered to be statistically significant.

Results

qPCR indicates IL-1β- and Erastin-induced changes in Sat1 expression

We tested various in vitro pathological models and found that IL-1 and Erastin can cause a significant increase in Sat1. The quantitative polymerase chain reaction (qPCR) analysis we performed shows that Sat1 expression was increased in chondrocytes, induced by IL-1β and Erastin (Figure 1a).

Silencing Sat1 could reduce ECM degradation and inflammation

As a major component of the ECM, type II collagen (collagen II) is up-regulated after Sat1 silencing.[25] MMP13 and MMP3, the main degradation enzymes of the ECM, were significantly decreased after Sat1 silencing.[26] In addition, the expression of iNOS, which produces excessive NO in chondrocytes to promote cartilage destruction and cell damage,[27] was also decreased when Sat1 was silenced in chondrocytes (Figures 1b and 1d). We treated chondrocytes with Erastin instead of IL-1β, which also increased collagen II expression. MMP13, MMP3, and iNOS expression was reduced (Figures 1c and 1e). Thus, these results suggest that silencing Sat1 could alleviate ECM degradation and inflammation in chondrocytes.

Silencing Sat1 could attenuate chondrocyte ferroptosis

Considering that Sat1 is related to the ferroptotic process, we further examined its role in chondrocyte ferroptosis. The results revealed that ferroptosis-related protein expression was significantly changed when Sat1 was knocked-down in chondrocytes, evident by decreased SLC7A11 expression and increased expression of Alox15 and lpcat3 compared to the IL-1β treated group (Figures 2a and 2d). Consistently, the same changes occurred in chondrocytes that were treated with Erastin (Figures 2b and 2e).

We also measured the levels of ROS and lipid ROS; the results revealed that after treatment with IL-1β or Erastin, ROS and lipid ROS accumulated in chondrocytes (as indicated by green fluorescence intensity). Silencing of Sat1 reduced the ROS (Figures 1f and 1g) and lipid ROS (Figures 2f and 2g) levels. In addition, after treatment with IL-1β or erastin, the MDA was notably increased in chondrocytes while Sat1 knockdown reduced MDA levels (Figure 2c). These results indicate that Sat1 knockdown could attenuate the ferroptotic phenomenon in chondrocytes.

Knockdown of Alox15 could effectively protect chondrocytes against inflammation and ferroptosis

Alox15 is a member of the lipoxygenase family and is closely related to oxidative stress-related cell death.[28] The expression level of Alox15 upregulated by Sat1, and a high level of Alox15 induces ROS production.[29] In this study, Alox15 knockdown caused increased expression of collagen II and decreased expression of MMP13, MMP3, and iNOS (Figures 3a and 3c). In addition, knockdown of Alox15 upregulated the expression of SLC7A11 (Figures 3e and 3g). Moreover, a similar change in expression of collagen II, SLC7A11, MMP13, MMP3, and iNOS was observed in Alox15 knocked-down chondrocytes exposed to Erastin (Figures 3b, 3d, 3f, and 3h). Taken together, our results demonstrate that knocking down Alox15 can alleviate ferroptosis and ECM degradation of chondrocytes.

Sat1-Alox15 axis regulates Nrf2 signalling in chondrocytes

As a critical antioxidant system in cells, the Nrf2 pathway is essential for the attenuation of lipid peroxidation and ferroptosis.[30] Therefore, the possible role of Nrf2 on SAT-mediated ferroptosis was investigated. The results revealed that expression of Nrf2, HO-1, and NQO1 was significantly increased when Sat1 was knocked-down. GPX4 plays an important role in resisting lipid peroxidation. Interestingly, IL-1β treatment inhibited expression of GPX4, which could be reversed by knockdown of Sat1 (Figures 4a to 4d).

As a downstream target of Sat1, Alox15 knockdown also affects the Nrf2 pathway. Expression of Nrf2, NQO1, and GPX4 was increased after Alox15 was knocked-down in chondrocytes (Figures 5a to 5d).

Taken together, we found that the Sat1-Alox15 axis regulates the Nrf2 pathway, indicating that Nrf2 may regulate the Sat1-Alox15 axis.

Nrf2 mediated role of Sat1-Alox15 axis in chondrocyte ferroptosis

To verify the relationship between Nrf2 and the Sat1-Alox15 axis further, we knocked-down Alox15 and Nrf2 at the same time. Western blot results showed that knockdown of Alox15 caused the downregulation of iNOS, MMP3, and upregulation of Nrf2 signalling, all of which were reversed by knockdown of Nrf2. These findings confirm our prediction that knocking down the Sat1-Alox15 axis could protect chondrocytes via activation of the Nrf2 pathway (Figures 6a to 6d).

DA inhibits Sat1 expression and protects chondrocytes

Considering the chondroprotective effects of Sat1-Alox15 axis inhibition, we sought to explore the therapeutic potential by targeting this axis. Through a literature search, we found that DA could effectively inhibit Sat1 expression.[31] Therefore, we used the concentration of DA reported in the literature (200 μM) to treat chondrocytes in vitro. Firstly, we stained the cells with toluidine blue, which showed that 100 μM and 200 μM DA did not significantly affect cell morphology (Figure 7e). CCK-8 assay was performed and cell activity was promoted by DA treatment (100 μM and 200 μM) (Figure 7d). Western blot analysis revealed that DA inhibits the increase in MMP13, MMP3, Alox15, iNOS, and Sat1 expression and lessens the decrease in collagen II expression induced by IL-1β (Figures 7b and 7c).

DA alleviated cartilage degeneration and increased the expression of collagen II in a mouse OA model

We carried out an experiment in vivo to evaluate the therapeutic effects of DA on OA progression. As referred to the concentration of DA used in the literature, we chose 3 mg/kg and 30 mg/kg for the in vivo experiment.[31] DMM surgery was performed on eight-week-old mice to induce the OA model, which was followed by intra-articular injection of DA. The safranin O/fast green staining results showed that DMM mice treated with the 3 mg/kg DA showed improved cartilage degeneration with a lower OARSI score compared to the DMM group (Figures 8c and 8d).

In addition, we observed that osteophyte formation was reduced and bone loss in tibial platform was ameliorated, as shown by 3D modelling (Figures 8a and 8b). Surprisingly, the high concentration of DA did not reverse the OA damage caused by DMM surgery. Immunohistochemistry analysis showed that Sat1 and Alox15 levels in the DMM group were significantly reduced, but only the low concentration group had restored expression of type II collagen, which was consistent with the results observed by safranin O/fast green staining (Figures 8f and 8g).

Discussion

Over the past few years, ferroptosis has received increasing attention for its involvement in the pathogenesis of OA. Previous research has focused on the alteration of iron homeostasis and ferroptosis on OA,[32,33] but the relationship between Sat1-Alox15, the core lipid peroxidation process in ferroptosis, and OA is still unclear. In this project, we attempted to establish a connection between Sat1-ALXO15 and OA. We determined that the elevation of Sat1 and Alox15 would inhibit the Nrf2 pathway, leading to an increase in the intracellular oxidation level and accumulation of lipid peroxidation, ultimately aggravating the destruction of cartilage. Therefore, maintaining the level of lipid peroxidation by inhibiting the Sat1-Alox15 axis may be a new treatment strategy for OA.

Nrf2, the major molecule of the cellular antioxidant system, is released from its inhibitor Keap1 and then regulates the level of antioxidant genes, including HO-1 and NQO1, in response to stress.[34] Nrf2 is a key protective factor against inflammation and ferroptosis.[35] In our study, inhibiting Sat1 and Alox15 activated the Nrf2 pathway, inhibited oxidative stress, and protected chondrocytes from ferroptosis. In order to explore the relationship between Nrf2 and the Sat1-Alox15 axis, we also knocked down two key factors, Alox15 and Nrf2. It can be seen that after knocking down these two factors at the same time, the inflammation and ferroptosis of chondrocytes are not relieved, the expression of inflammation-related index collagen II is reduced, MMP3 and iNOS is increased. Besides, the expression of ferroptosis-related indicators GPX4 and SLC7A11 is decreased. This proves our previous conjecture that after knocking out Alox15, the Nrf2 pathway that should have been activated was artificially cut off, and its protective effect decreased, leading to increased chondrocyte inflammation and ferroptosis. The results indicate that the Nrf2-mediated antioxidant system is crucial for the survival of chondrocytes, and the Sat1-Alox15 axis aggravates chondrocyte ferroptosis by inhibiting Nrf2. This study therefore established a connection between Nrf2 and SAT-Alox15 in the OA modeland may provide more precise strategies for the treatment of OA.

To further verify this hypothesis, we carried out DA in vivo experiments. DA is an aromatic diamidine compound generated by Surfen C. In recent decades, DA has been used as an antitrypsin inhibitor.[36] Extensive research has shown that DA has potential benefits in the treatment of animal models of diseases such as asthma, gastric disease, and ischaemic stroke.[37-40] Recent studies have demonstrated that DA could also inhibit Sat1 and thereby play a therapeutic role.[29,41] Through the results of safranin O/fast green staining and immunohistochemical analysis, we can observe that the progression of OA in mice that received 3 mg/kg injections was alleviated, osteophyte formation was reduced, and the destruction of the tibial platform was ameliorated. There were no differences in response to the different treatments in vitro, which verified our hypothesis.

Our research still has some limitations. First, the literature shows that DA is not a specific inhibitor of Sat1, and the solubility of DA is not suitable for intra-articular injection, leading to OA not being alleviated in the high concentration group. We showed that inhibiting Sat1 could alleviate OA. Since no specific inhibitor of Sat1 has been found, the development of these drugs may provide more precise strategies for the treatment of OA. Second, our research could not determine whether the elimination of Sat1 led to the recovery of Nrf2 or whether the reduction in ferroptosis led to the recovery of Nrf2, and further research is needed to verify whether there is a link between Sat1 and Nrf2.

In conclusion, we showed that knocking out Sat1 and its downstream target Alox15 could increase the expression of Nrf2, effectively alleviate lipid peroxidation, and alleviate the damage to chondrocytes caused by ferroptosis and inflammation. Sat1 therefore seems to be a novel target for subsequent research on OA.

Supplementary material

ARRIVE checklist

References

1. **Glyn-Jones S**, **Palmer AJR**, **Agricola R**, **et al**. Osteoarthritis. *Lancet*. 2015;386(9991):376–387.
2. **Hunter DJ**, **Bierma-Zeinstra S**. Osteoarthritis. *Lancet*. 2019;393(10182):1745–1759.
3. **Musumeci G**, **Aiello FC**, **Szychlinska MA**, **Di Rosa M**, **Castrogiovanni P**, **Mobasheri A**. Osteoarthritis in the XXIst century: risk factors and behaviours that influence disease onset and progression. *Int J Mol Sci*. 2015;16(3):6093–6112.
4. **Mobasheri A**, **Batt M**. An update on the pathophysiology of osteoarthritis. *Ann Phys Rehabil Med*. 2016;59(5–6):333–339.
5. **Abramoff B**, **Caldera FE**. Osteoarthritis: pathology, diagnosis, and treatment options. *Med Clin North Am*. 2020;104(2):293–311.
6. **Gozzelino R**, **Arosio P**. Iron homeostasis in health and disease. *Int J Mol Sci*. 2016;17(1):130.
7. **Li C**, **Ouyang N**, **Wang X**, **et al**. Association between the ABO blood group and primary knee osteoarthritis: a case-control study. *J Orthop Translat*. 2020;21(129):129–135.
8. **Sellam J**, **Berenbaum F**. The role of synovitis in pathophysiology and clinical symptoms of osteoarthritis. *Nat Rev Rheumatol*. 2010;6(11):625–635.

9. **Sandell LJ**, **Aigner T**. Articular cartilage and changes in arthritis. An introduction: cell biology of osteoarthritis. *Arthritis Res*. 2001;3(2):107–113.
10. **Luo P**, **Yuan Q-L**, **Yang M**, **Wan X**, **Xu P**. The role of cells and signal pathways in subchondral bone in osteoarthritis. *Bone Joint Res*. 2023;12(9):536–545.
11. **Jiang S**, **Liu Y**, **Xu B**, **Zhang Y**, **Yang M**. Noncoding RNAs: New regulatory code in chondrocyte apoptosis and autophagy. *Wiley Interdiscip Rev RNA*. 2020;11(4):e1584.
12. **Dixon SJ**, **Lemberg KM**, **Lamprecht MR**, **et al**. Ferroptosis: an iron-dependent form of nonapoptotic cell death. *Cell*. 2012;149(5):1060–1072.
13. **Seibt TM**, **Proneth B**, **Conrad M**. Role of GPX4 in ferroptosis and its pharmacological implication. *Free Radic Biol Med*. 2019;133:144–152.
14. **Yao X**, **Sun K**, **Yu S**, **et al**. Chondrocyte ferroptosis contribute to the progression of osteoarthritis. *J Orthop Translat*. 2021;27:33–43.
15. **Sun K**, **Hou L**, **Guo Z**, **et al**. JNK-JUN-NCOA4 axis contributes to chondrocyte ferroptosis and aggravates osteoarthritis via ferritinophagy. *Free Radic Biol Med*. 2023;200:87–101.
16. **Lewerenz J**, **Hewett SJ**, **Huang Y**, **et al**. The cystine/glutamate antiporter system x(c)(-) in health and disease: from molecular mechanisms to novel therapeutic opportunities. *Antioxid Redox Signal*. 2013;18(5):522–555.
17. **Jiang L**, **Kon N**, **Li T**, **et al**. Ferroptosis as a p53-mediated activity during tumour suppression. *Nature*. 2015;520(7545):57–62.
18. **Ou Y**, **Wang SJ**, **Li D**, **Chu B**, **Gu W**. Activation of SAT1 engages polyamine metabolism with p53-mediated ferroptotic responses. *Proc Natl Acad Sci U S A*. 2016;113(44):E6806–E6812.
19. **Li J**, **Cao F**, **Yin H-L**, **et al**. Ferroptosis: past, present and future. *Cell Death Dis*. 2020;11(2):88.
20. **Khan NM**, **Ahmad I**, **Haqqi TM**. Nrf2/ARE pathway attenuates oxidative and apoptotic response in human osteoarthritis chondrocytes by activating ERK1/2/ELK1-P70S6K-P90RSK signaling axis. *Free Radic Biol Med*. 2018;116:159–171.
21. **Khan NM**, **Haseeb A**, **Ansari MY**, **Devarapalli P**, **Haynie S**, **Haqqi TM**. Wogonin, a plant derived small molecule, exerts potent anti-inflammatory and chondroprotective effects through the activation of ROS/ERK/Nrf2 signaling pathways in human osteoarthritis chondrocytes. *Free Radic Biol Med*. 2017;106:288–301.
22. **Kumar H**, **Kim I-S**, **More SV**, **Kim B-W**, **Choi D-K**. Natural product-derived pharmacological modulators of Nrf2/ARE pathway for chronic diseases. *Nat Prod Rep*. 2014;31(1):109–139.
23. **Sun K**, **Luo J**, **Jing X**, **et al**. Astaxanthin protects against osteoarthritis via Nrf2: a guardian of cartilage homeostasis. *Aging (Albany NY)*. 2019;11(22):10513–10531.
24. **Bannuru RR**, **Osani MC**, **Vaysbrot EE**, **et al**. OARSI guidelines for the non-surgical management of knee, hip, and polyarticular osteoarthritis. *Osteoarthritis Cartilage*. 2019;27(11):1578–1589.
25. **Morales-Ivorra I**, **Romera-Baures M**, **Roman-Viñas B**, **Serra-Majem L**. Osteoarthritis and the Mediterranean diet: a systematic review. *Nutrients*. 2018;10(8):1030.
26. **Vincenti MP**, **Brinckerhoff CE**. Transcriptional regulation of collagenase (MMP-1, MMP-13) genes in arthritis: integration of complex signaling pathways for the recruitment of gene-specific transcription factors. *Arthritis Res*. 2002;4(3):157–164.
27. **Anavi S**, **Tirosh O**. iNOS as a metabolic enzyme under stress conditions. *Free Radic Biol Med*. 2020;146:16–35.
28. **Seiler A**, **Schneider M**, **Förster H**, **et al**. Glutathione peroxidase 4 senses and translates oxidative stress into 12/15-lipoxygenase dependent- and AIF-mediated cell death. *Cell Metab*. 2008;8(3):237–248.
29. **Neidhart M**, **Karouzakis E**, **Jüngel A**, **Gay RE**, **Gay S**. Inhibition of spermidine/spermine N1-acetyltransferase activity: a new therapeutic concept in rheumatoid arthritis. *Arthritis Rheumatol*. 2014;66(7):1723–1733.
30. **Dodson M**, **Castro-Portuguez R**, **Zhang DD**. NRF2 plays a critical role in mitigating lipid peroxidation and ferroptosis. *Redox Biol*. 2019;23:101107.
31. **Ge P**, **Yao X**, **Li J**, **Jiang R**, **Dai J**, **Zhang L**. Diminazene aceturate alleviated lipopolysaccharide/D-galactosamine-induced fulminant hepatitis in mice. *Biomed Pharmacother*. 2018;98:142–148.
32. **Guo Z**, **Lin J**, **Sun K**, **et al**. Deferoxamine alleviates osteoarthritis by inhibiting chondrocyte ferroptosis and activating the Nrf2 pathway. *Front Pharmacol*. 2022;13:791376.
33. **Lin J**, **Guo Z**, **Zheng Z**, **et al**. Desferoxamine protects against hemophilic arthropathy through the upregulation of HIF-1α-BNIP3 mediated mitophagy. *Life Sci*. 2023;312:121172.
34. **Cuadrado A**, **Rojo AI**, **Wells G**, **et al**. Therapeutic targeting of the NRF2 and KEAP1 partnership in chronic diseases. *Nat Rev Drug Discov*. 2019;18(4):295–317.
35. **Sun K**, **Luo J**, **Jing X**, **et al**. Hyperoside ameliorates the progression of osteoarthritis: an in vitro and in vivo study. *Phytomedicine*. 2021;80:153387.
36. **Peregrine AS**, **Mamman M**. Pharmacology of diminazene: a review. *Acta Trop*. 1993;54(3–4):185–203.
37. **Dhawale VS**, **Amara VR**, **Karpe PA**, **Malek V**, **Patel D**, **Tikoo K**. Activation of angiotensin-converting enzyme 2 (ACE2) attenuates allergic airway inflammation in rat asthma model. *Toxicol Appl Pharmacol*. 2016;306:17–26.
38. **Souza LKM**, **Nicolau LAD**, **Sousa NA**, **et al**. Diminazene aceturate, an angiotensin-converting enzyme II activator, prevents gastric mucosal damage in mice: role of the angiotensin-(1-7)/Mas receptor axis. *Biochem Pharmacol*. 2016;112:50–59.
39. **Bennion DM**, **Haltigan EA**, **Irwin AJ**, **et al**. Activation of the neuroprotective angiotensin-converting enzyme 2 in rat ischemic stroke. *Hypertension*. 2015;66(1):141–148.
40. **Zheng C**, **Lei C**, **Chen Z**, **et al**. Topical administration of diminazene aceturate decreases inflammation in endotoxin-induced uveitis. *Mol Vis*. 2015;21:403–411.
41. **Libby PR**, **Porter CW**. Inhibition of enzymes of polyamine back-conversion by pentamidine and berenil. *Biochem Pharmacol*. 1992;44(4):830–832.

Author information

J. Xu, MMed, Researcher
Z. Ruan, MMed, Researcher
Z. Guo, MD, Researcher
L. Hou, MD, Researcher
G. Wang, MD, Researcher
Z. Zheng, MD, Researcher
X. Zhang, MMed, Researcher
H. Liu, MD, Researcher
K. Sun, MD, Orthopaedic Surgeon
F. Guo, PhD, Orthopaedic Surgeon
Department of Orthopedics, Tongji Hospital, Tongji Medical College, Huazhong University of Science and Technology, Wuhan, China.

Author contributions

J. Xu: Conceptualization, Data curation, Formal analysis, Investigation, Writing – original draft.
Z. Ruan: Data curation, Formal analysis, Methodology, Writing – original draft.
Z. Guo: Formal analysis, Methodology, Data curation.
L. Hou: Data curation, Formal analysis.
G. Wang: Investigation, Data curation.
Z. Zheng: Formal analysis.
X. Zhang: Validation.
H. Liu: Visualization.
K. Sun: Methodology, Project administration, Writing – review & editing.
F. Guo: Project administration, Writing – review & editing.

Funding statement

The authors disclose receipt of the following financial or material support for the research, authorship, and/or publication of this article: funding from the National Natural Science Foundation of China (No. 82172498 and No. 82102625).

Data sharing

The data that support the findings for this study are available to other researchers from the corresponding author upon reasonable request.

Acknowledgements

The authors wish to thank the National Natural Science Foundation of China for funding assistance with this research, and also thank all the personnel involved in the experiments for their efforts.

Ethical review statement

The experimental procedures involving animals were ethically approved by the Experimental Animal Ethics Committee of Tongji Medical College, Huazhong University of Science and Technology, Wuhan, China.

Open access funding

The authors report that they received open access funding for their manuscript from the National Natural Science Foundation of China (No. 82172498 and No. 82102625).